

Fabrication of nanodiamond-based composite monolithic column and its application in separation of small molecules

A. L. Wei,^{1,2} H. Y. Liu,^{1,2} F. Q. Wang,^{1,2} X. Y. Li,^{1,2} H. Y. Yan^{1,2}

¹College of Pharmaceutical Sciences, Hebei University; Key Laboratory of Pharmaceutical Quality Control of Hebei Province, Baoding, 071002, China

²Key Laboratory of Medicinal Chemistry and Molecular Diagnosis, Ministry of Education, Baoding, 071002, China

Correspondence to: H. Y. Liu (E-mail: lhy1610@126.com)

ABSTRACT: A nanodiamond-based composite monolithic column was fabricated by redox initiation for high-performance liquid chromatography. In the fabrication process, functionalized nanodiamond was used as the functional monomer, dipentaerythritol hexaacrylate and 1,10-decanediol diacrylate as cross-linking agents, polyethylene glycol 400 and 1-propanol as coporogens, and dibenzoyl peroxide and *N,N*-dimethyl aniline as initiators. Compared to polymer monolithic columns without nanodiamond, a nanodiamond-based composite monolithic column prepared under the same conditions exhibited relatively high resolution and efficiency. Characterizations of the resulting nanocomposite were carried out, including scanning electron microscopy, mercury intrusion porosimetry, nitrogen adsorption-desorption isotherm measurement, and thermogravimetric analysis. The ND-based composite monolith exhibited a uniform and reticular skeleton microstructure, thermal stability, and mechanical stability. In addition, the nanodiamond-based composite monolithic column was used to separate a series of small molecules with good resolution and reproducibility in high-performance liquid chromatography. © 2016 Wiley Periodicals, Inc. *J. Appl. Polym. Sci.* **2016**, *133*, 43776.

KEYWORDS: composites; nanoparticles; nanowires and nanocrystals; porous materials; properties and characterization; separation techniques

Received 13 December 2015; accepted 10 April 2016

DOI: 10.1002/app.43776

INTRODUCTION

Nanodiamond (ND) is a kind of carbon-based nanoparticle bringing diamond properties into the nanoscale material world,¹ and it was created by nuclear explosions that used carbon-based trigger explosives by Russian scientists in the 1960s.² In recent decades, ND has aroused considerable scientific interest in the field of carbon nanomaterials such as graphene oxide,³ carbon nanofiber, and carbon nanotubes.^{4,5} ND particles possess many unique properties, including superior thermal conductivity; high hardness, Young's modulus, and resistivity; chemical inertness; good electrical insulating properties; and a high refractive index.⁶ It is demonstrated that nanodiamond clusters become more stable than graphitic polyaromatics with the increased hydrogen-to-carbon ratio and the crossover in stability occurring at nanometer-scale radii, which was calculated at Los Alamos in 1990.⁷ Therefore, it is significant and worth functionalizing nanodiamond to control and tailor the surface chemistry and then combine with polymers to form polymer nanocomposites in order to optimize properties utilizing its own excellent character.⁸

So far, ND has been produced by detonation in large volumes at low cost, which brought about many new products, such as

composites,⁹ catalysts,¹⁰ and magnetic sensors.¹¹ ND composite itself has attracted much attention in industrial applications and medical fields and has been applied in many fields. Silva and coworkers synthesized a micro- and nanodiamond composite for the photocatalytic degradation of environmental water pollutants.⁹ Gogotsi and coworkers applied fluorescent PLLA-nanodiamond composites for bone tissue engineering.¹² It was also an important work that nanocomposites were conducted on a wide variety of combinations together with polymers (epoxy resins, phenolics and so on) and porous composite structures generated from multiphase polymer blends, as was studied by Baklavaridis and coworkers.¹³

Monolithic stationary phases play an extremely important role in high-performance liquid chromatography. They have developed rapidly because of their unique properties, such as cost-effectiveness, simple preparation, low back pressure, fast mass transfer kinetics, and versatile surface modification compared to conventional columns packed with particles.^{14,15} Additionally, another property of monolithic columns is that through-pore size and skeletal structure can be varied nonlinearly, which contributes to reducing mass transfer resistance and increasing column permeability.

Table I. Compositions of the Polymerization Mixtures for the Composite Monoliths Prepared in This Study

Column	ND (mg)	Cross-linker component (% w/w)		Porogen component (% v/v)		BPO (mg)	DMA (μ L)	Back pressure ^a (bar)	Permeability K ($\times 10^{-14}$ m ²)
		DPHA	DDA	PEG-400	Propanol				
A	0	20	80	28	72	5	50	2	9.5
B	2	20	80	28	72	5	50	4	4.75
C	3	20	80	28	72	5	50	No dispersing of ND	— ^b
D	2	26	74	28	72	5	50	>11	—
E	2	13	87	28	72	5	50	7	2.71
F	2	20	80	20	80	5	50	>10	—
G	2	20	80	36	64	5	50	3	6.33

^aBack pressure is obtained with ACN as the mobile phase at 1 mL/min, and the length of the stainless steel column was kept at 5 cm.

^bThe columns have no permeability data.

In this study, considering the superior qualities of ND, ND particles via chemical modification were used as a functional monomer. An ND-based polymer composite was prepared and used as a monolithic stationary phase to separate a mixture of acidic, alkaline, and neutral compounds, at the same time achieving 19,740 plates per meter.

EXPERIMENTAL

Materials

Dipentaerythritol hexaacrylate (DPHA) and 1,10-decanediol diacrylate (DDA) were provided by Liyang Runda Co. Ltd. (Liyang, China). The material 3-methacryloxypropyltrimethoxysilane (KH-570) was purchased from Macklin Co. Ltd. (Shanghai, China). ND (50 nm) was produced by Xuzhou Jiechuang New Material Technology Co. Ltd. (Xuzhou, China). High-performance liquid chromatography (HPLC)-grade methanol and acetonitrile were provided by Kermel Chemical Reagent Co. Ltd. (Tianjin, China). Polyethylene glycol 400 (PEG-400), 1-propanol, dibenzoyl peroxide (BPO), *N,N*-dimethyl aniline (DMA), FeSO₄·H₂O, H₂O₂, H₂SO₄, and ethanol were obtained from Tianjin Guangfu Chemical Co. Ltd. (Tianjin, China). Aromatic compounds were purchased from Beijing Chemical Plant (Beijing, China). All solutions were filtered through a 0.45 μ m membrane. The stainless-steel columns (50 \times 4.6 mm i.d.) were purchased from Beijing Xinyu Instrument Co. Ltd. (Beijing, China).

Instruments

All chromatographic experiments were carried out on a Dionex UltiMate 3000 from Thermo Fisher Scientific (Massachusetts, the United States). The sample injection volume of the auto-sampler was 10.0 μ L. Scanning electron microscopy (SEM) of the monoliths was carried out on a KYKY-2800B scanning electron microscope (Beijing, China) scanning electron microscope. The porosity was recorded by mercury intrusion porosimetry on an AutoPore IV 9500 Micromeritics (Atlanta, the United States), which had the ability to measure pore diameters from 0.003 to 360 μ m. The surface area was investigated on a Tristar II 3020 (Micromeritics). Thermogravimetric (TGA) measure-

ments were performed on a Setsys 16/18 (Setaram, Caluire, France). Standard solutions were prepared in acetonitrile (0.01–0.03 mg mL⁻¹) and stored at 4 °C in the dark.

Preparation of Hydroxylated ND

Briefly, FeSO₄·H₂O (6.95 g) was dissolved in ultrapure water and adjusted to pH 3 using H₂SO₄. Next, ND (0.1 g) and H₂O₂ (42.5 g) were mixed in the above solvent, and the mixture was refluxed for 5 h at 80 °C. After that, the NDs were separated by centrifuge and washed with water for several times to pH 6–7 and dried under vacuum for further use.

Functionalization of Hydroxylated ND

The OH functions of ND-OH can also be used for the reaction with oxophilic reagents such as trialkoxysilanes. Here, the same weight of hydroxylated nanodiamond and KH570 were mixed with 30 mL 95%(v/v) ethanol and reacted for 6 h at 60 °C with a mechanical stirrer and thermometer. Next, the nanodiamonds were separated by a centrifuge and washed with acetone in order to remove unreacted KH-570. Finally, the final nanodiamonds were evacuated in vacuum at 80 °C for 12 h.

Preparation of the poly(ND-co-DPHA-co-DDA) Composite Monolithic Column

A prepolymerization solution composed of monomer, cross-linking agent, porogen, and initiator was used to prepare the poly(ND-co-DPHA-co-DDA) monolith, as listed in Table I. In brief, this solution was made by dissolving various amounts of nanodiamond, DPHA, DDA, and BPO in a binary porogenic solvent, which consisted of PEG-400 and propanol. The mixture solution was sonicated for 20 min after being shaken for 2 min and then bubbled with nitrogen for another 5 min to obtain a homogeneous solution and remove gases. Then DMA was added to the mixture, which was degassed with an ultrasonicator and poured into a steel column (50 mm \times 4.6 mm i.d.), which was sealed at both ends with closed column heads. The column was allowed to proceed at room temperature for 1.5 h. The schematic preparation of the functionalized ND and polymerization process is shown in Figure 1. After the polymerization, the monoliths with

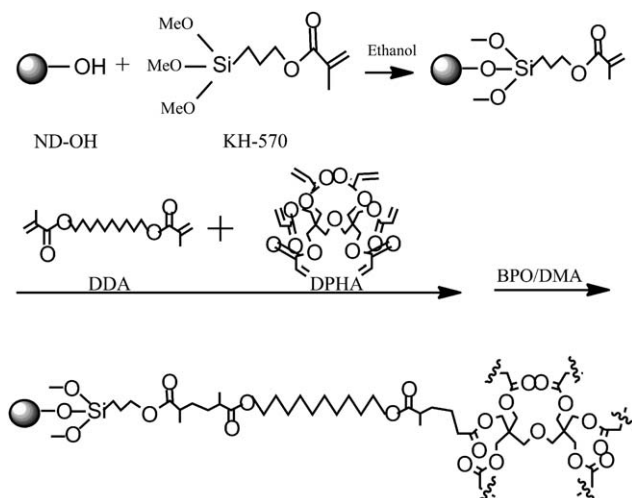


Figure 1. The schematic preparation of functionalized ND and the polymerization process.

the steel tube were eluted with methanol for 2 h at a flow rate of 1.0 mL/min to remove any residual monomers, porogens, and any other unreacted soluble compounds. The poly(DPHA-co-DDA) monolith was also prepared in the absence of nanodiamond by using the same preparation procedure.

Calculations

The ability of a liquid to pass through a material is expressed as permeability, which reflects through-pore size and external porosity. The permeability (K) of monolithic columns is calculated by Darcy's law:

$$K = F \times \eta \times L / \Delta P \times \pi \times r^2 \quad (1)$$

where F is the flow rate of the mobile phase, η is the dynamic viscosity of the mobile phase, L is the length of the column, ΔP is the back pressure of the column, π is the circumference ratio, and r is the inner radius of the column.¹⁶ In this work, acetonitrile (ACN) was used as the mobile phase, and its corresponding value of dynamic viscosity was 0.38 cP at 25 °C.¹⁷

The retention factor (k) of each aromatic compound is defined by the equation

$$k = (t_R - t_0) / t_0 \quad (2)$$

where k , t_0 , and t_R stand for the retention factor, the retention time of aromatic compounds, and the retention time of the void marker, respectively. Thiourea was selected as the void time marker in this experiment.

The theoretical plate number (N), one of the parameters of the chromatographic column efficiency, is a quantitative representation that indicates the separation efficiency. This equation was used to calculate the plate number:

$$N = 5.55(t_R / W_{0.5}) / L \quad (3)$$

where N is the theoretical plate number per m, t_R is the retention time of the analyte in min, $W_{0.5}$ is the peak width at half height in min, and L is the length of the column.¹⁸

Characterization

First, the permeability and mechanical strength of the composite monolith was evaluated by the back pressure at different flow rates with ACN and water as the mobile phase. Furthermore, to observe the morphology of the resulting monolith, the monolithic materials were pushed out of the stainless steel column and cut into small pieces and then dried in a vacuum at 60 °C for 24 h. Then, a small fragment of monolith was used for SEM. Finally, the pore size distribution, pore types, and thermal stability were tested by mercury intrusion porosimetry, a nitrogen adsorption-desorption instrument, and thermogravimetric measurements, respectively.

RESULTS AND DISCUSSION

Preparation

Covering the nanodiamond's surface with OH groups is a surface-modification technique. Hydroxyl functions provide a broad variety of subsequent reactions. Several approaches have been reported so far. A highly efficient method for the direct establishment of OH groups on the ND surface consists of the reaction of pristine nanodiamond with the so-called Fenton reagent, which consists of hydrogen peroxide and FeSO₄ in a strongly acidic solution. Garcia and coworkers reported the successful oxidation of detonation nanodiamond with Fenton reagent.^{19,20} In the study, hydroxylated nanodiamond was prepared using this reagent.

In the preparation of the monolith, dipentaerythritol hexaacrylate (DPHA) is a polyolacrylate that possesses six double bonds with high reactivity, which can capture free radicals easily to form a dense skeletal structure that can be used as an important cross-linker. 1,10-Decanediol diacrylate (DDA), which has long carbon chains, is also a cross-linker combined with DPHA as a binary cross-linker. It could be considered a good solvent because its solubility value is similar to that of the monomer, which helps in obtaining a monolith with low permeability and small pore size. Generally, small pore size or low column permeability is a result of delayed phase separation in the polymerizing reaction mixture, which is beneficial for fabricating efficient monoliths. However, a prolonged delay in phase separation results in macroscopically visible noncontinuous monoliths. Considering the solubility parameters of the porogens and after a series of tests, PEG400 and propanol were chosen as coporogens. In addition, in this work, a redox initiator was used to prepare a monolithic column, which occurred quickly under contact pressure and ambient temperature conditions. It has several advantages: reduction of the activation energy of organic peroxide decomposition, effective control of the reaction rate, a complete curing reaction, and good mechanical stability of the products. In the initiator system, *N,N*-dimethyl aniline was the reducing agent, and benzoyl peroxide could initiate the polymerization of vinyl monomers.

Characterization of Poly(ND-co-DPHA-co-DDA) Monoliths

Morphology and SEM Study of the Monolith. The composition of the polymerization mixtures played an important role in the structure of the monolith. Several parameters are listed in Table I, including the compositions of monomers, cross-linkers, and porogens. Figure 2 shows several corresponding SEM

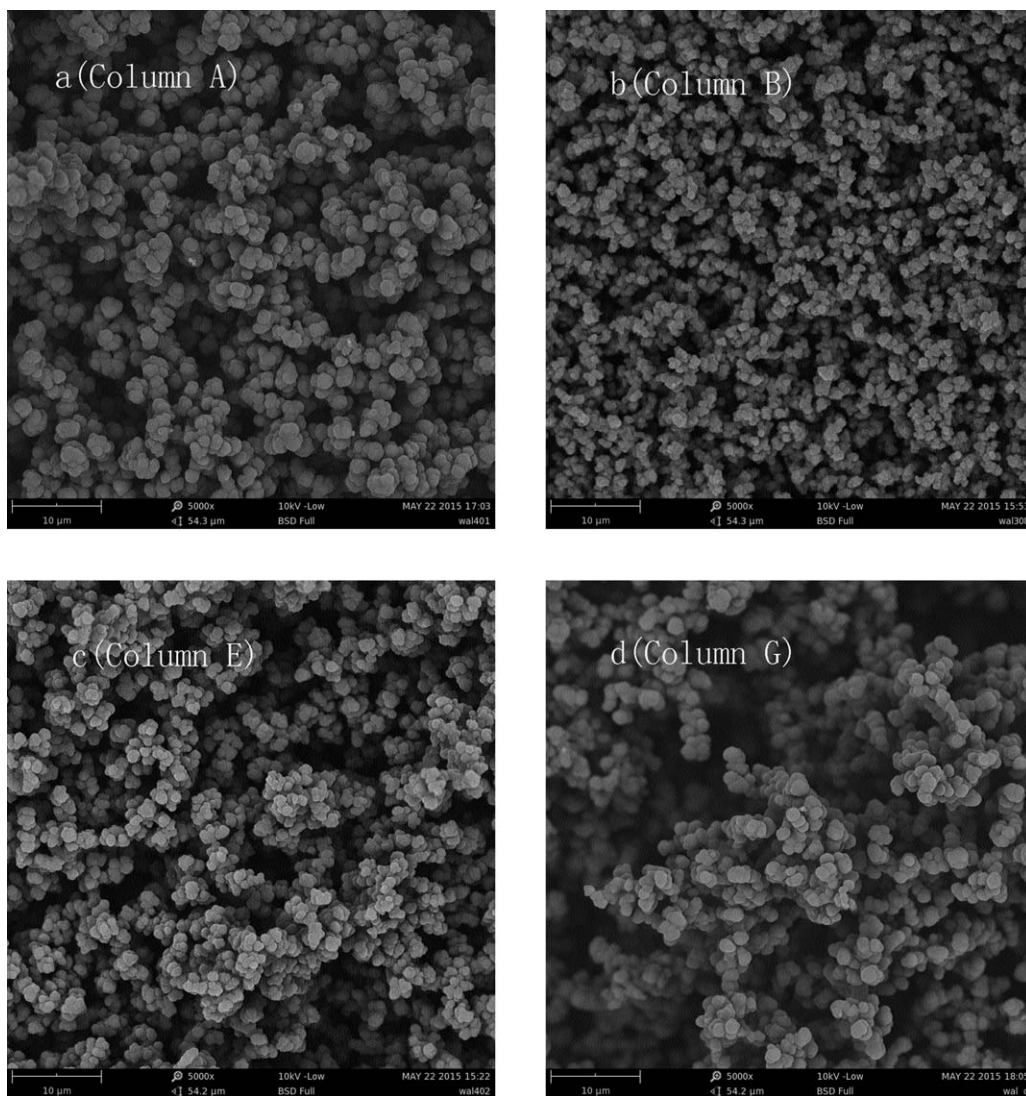


Figure 2. SEM micrographs of different monoliths.

micrographs of the porous structure of the different monoliths. When increasing the amount of DPFA, monolith B showed a more uniform skeleton and dense pore structure, as seen by comparing with column E [Figure 2(c)]. In Figure 2(d) (column G), a large number of microglobules were aggregated into large clusters, and large irregular through-pores were obtained by changing the ratio of porogens. Compared to column B [Figure 2(b)], the structure of column A [Figure 2(a)] without nanodiamond exhibited relatively looser. In addition, as noted in Table I, columns D and F collapsed easily, so they could not afford the pressure test. Based on the observations above, the compositions of column B were selected for all further tests.

The pore size distribution was investigated by mercury intrusion porosimetry. Based on Figure 3, the total intrusion volume, average pore diameter, and the porosity were 2.47 mL g^{-1} , $0.80 \mu\text{m}$, and 72.05%, respectively. The results revealed that the composite monolith possessed a macroporous structure, low back pressure, high permeability, and fast mass transfer.

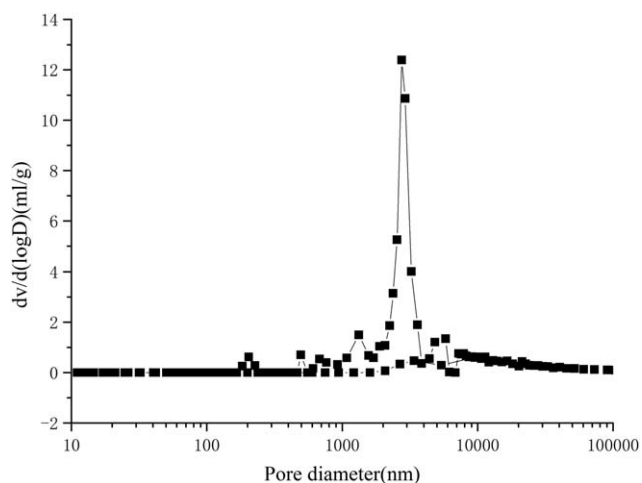


Figure 3. The measurement of pore size distribution for ND-based composite by mercury intrusion porosimetry.

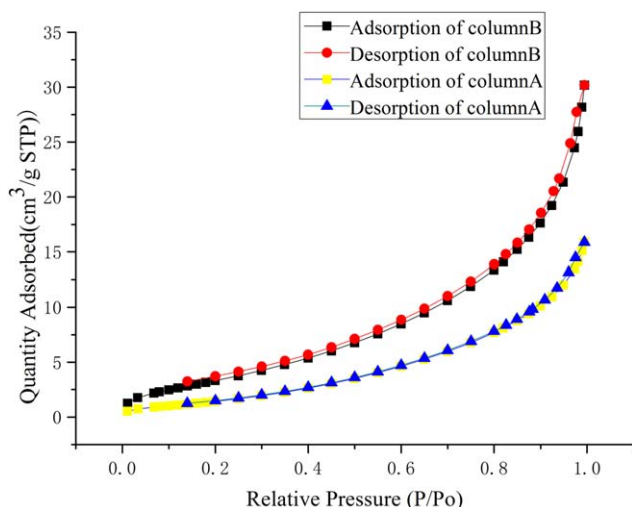


Figure 4. Nitrogen adsorption–desorption isotherm of polymer monolith without ND (column A) and with ND-based composite (column B). [Color figure can be viewed in the online issue, which is available at wileyonlinelibrary.com.]

Nitrogen adsorption–desorption isotherms were used to estimate the total surface area of the porous monolith. As shown in Figure 4, the nitrogen adsorption–desorption isotherm of column A and B exhibited typical type-III hysteresis, which demonstrated the strong interaction between the adsorption material and adsorbent. The total surface area of the ND-based composite monolith was $13.67 \text{ m}^2 \text{ g}^{-1}$, which was higher than that obtained from the polymer without ND ($8.74 \text{ m}^2 \text{ g}^{-1}$).

Mechanical Strength and Permeability. As shown in Figure 5, the measured back pressure is plotted against the flow rate, and good linearity (correlation coefficient $r > 0.99$) is achieved, which indicated that the composite monolith possessed good mechanical stability. When the flow rate was 1.0 mL min^{-1} , the permeability value calculated based on the law was $4.75 \times 10^{-14} \text{ m}^2$.

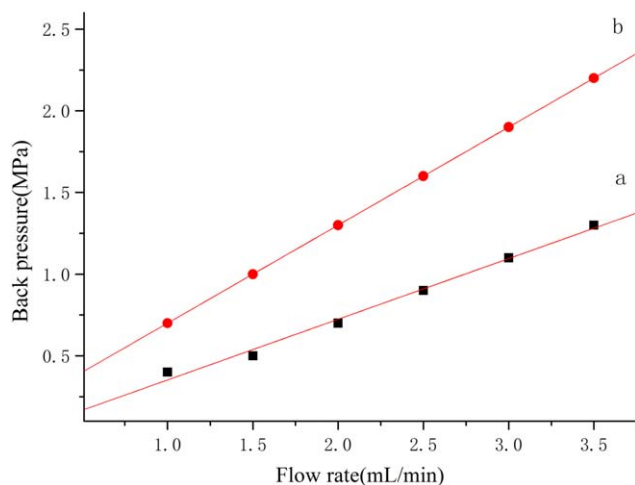


Figure 5. Effect of mobile phase flow rate on the pressure of column B; mobile phase: (a) ACN and (b) water. [Color figure can be viewed in the online issue, which is available at wileyonlinelibrary.com.]

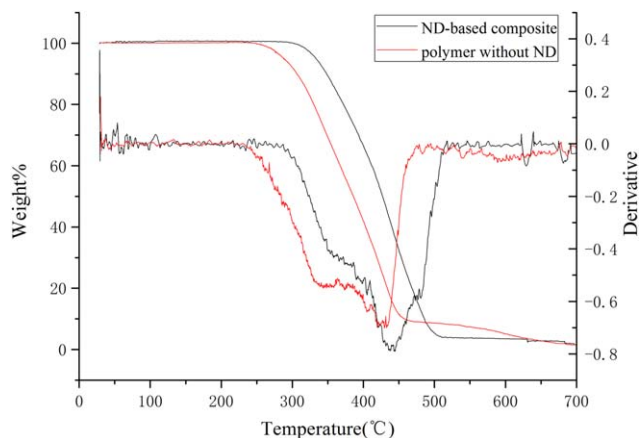


Figure 6. Thermogravimetric measurements of monolith with and without ND. [Color figure can be viewed in the online issue, which is available at wileyonlinelibrary.com.]

Thermostability of the Composite Monolith. The thermogravimetric measurement is an important parameter to evaluate the thermostability of a monolith. The TGA traces of the monoliths are shown in Figure 6. The TGA result of the ND-based composite monolith in weight loss was obtained at 300°C , which was higher than for the polymer monolith without ND at 245°C . The thermal stability of the polymer could be improved by the addition of ND powder because ND powder was a barrier to hinder the volatile decomposition products throughout the composites.

Chromatographic Character of the Monolith

In order to investigate the differences between the addition and absence of functional ND, three aromatic hydrocarbons were separated by column A and column B under the same chromatography conditions. The preparation conditions and prepolymerization solution component of column A were the same as for column B except for the absence of ND. As shown in Figure 7(A), the peaks of diphenyl and phenanthrene were lapped on column A, while a baseline separation was obtained on column B. The compounds eluted in the order of benzene, diphenyl, and phenanthrene according to the hydrophobicity, indicating a typical reversed-phase retention mechanism. To further examine the reversed-phase retention mechanism, the change of retention factor (k) over the methanol content on column B was investigated in HPLC. From Figure 7(B), it could be seen that the retention factor (k) decreased with the increase of methanol content ranging from 75% to 95%, which confirmed the typical reverse phase (RP) chromatographic property of the composite monolithic stationary phase toward the hydrophobic solutes.

The ND-based composite monolith column and polymer monolith without ND were used to separate three alkaline compounds. This can be seen in Figure 8. Compared to column A, three analytes were baseline-separated by column B with ACN/water (v/v, 65/35) and obtained much better chromatographic performance. The analytes were eluted in the order of *p*-nitroaniline, 1-naphthylamine, and diphenylamine within 3.5 min, corresponding to their hydrophobicity (octanol–water coefficient, $\log P$) (the $\log P$ values are 1.39, 2.25, and 3.5, respectively) from low to

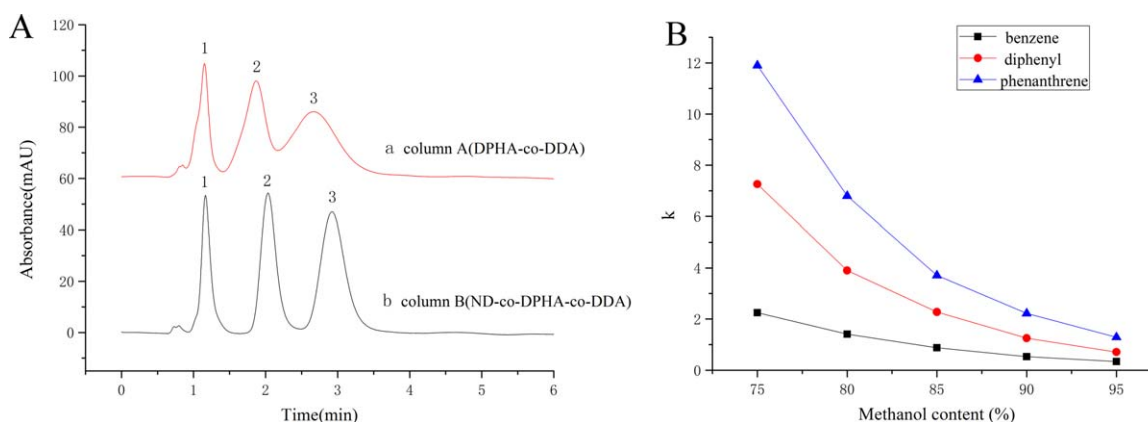


Figure 7. (A) Separation of benzene, biphenyl, and phenanthrene in order with (a) the poly(DPHA-co-DDA) monolith and (b) the poly(ND-co-DPHA-co-DDA) composite monolith; separation conditions: methanol/water (85/15, v/v) at a flow rate of 1 mL/min; detection wavelength, 254 nm. (B) Relationship between retention factor and methanol concentration of neutral compounds on column B. [Color figure can be viewed in the online issue, which is available at wileyonlinelibrary.com.]

high. The results indicated that the mode of separation was a typical reversed-phase retention mechanism.

To further study the potential of the ND-based composite monolith, a mixture of seven analytes that contained acidic, alkaline, and neutral compounds was separated. As shown in Figure 9, the seven compounds were eluted within 15 min, which confirmed that the composite monolith column possessed good separation character for acidic, alkaline, and neutral compounds. The theoretical plates were between 13,100 and 19,740 per meter.

Comparison with Other Polymer Monoliths

A large number of successful research studies on polymer monolithic columns have been reported. However, it was difficult to achieve high separation performance for small molecules in HPLC, which was relative easy to obtain for capillary liquid

chromatography (CLC) and capillary electro chromatography (CEC). Butyl methacrylate,²¹ lauryl methacrylate,²² and so on were the typical monomers used to separate small molecules, achieving about 15,000 plates per meter. Moreover, in our previous work, many polymer monolithic columns have been prepared using trimethylol propane triacrylate,²³ 1-dodecene,²⁴ and so on as monomers. Nevertheless, the previous column efficiency was not satisfactory and could not separate the mixture of acidic, alkaline, and neutral compounds at the same time. Here, a poly(ND-co-DPHA-co-DDA) composite monolithic column was prepared that exhibited good separation of acidic, alkaline, and neutral compounds, and its efficiency reached 19,740 plates per meter. It is a promising composite monolith for CLC and CEC in order to obtain better results in the future.

Monolithic Column Reproducibility and Stability

The reproducibility of the ND-based composite monolithic column was assessed by measuring the relative standard deviations

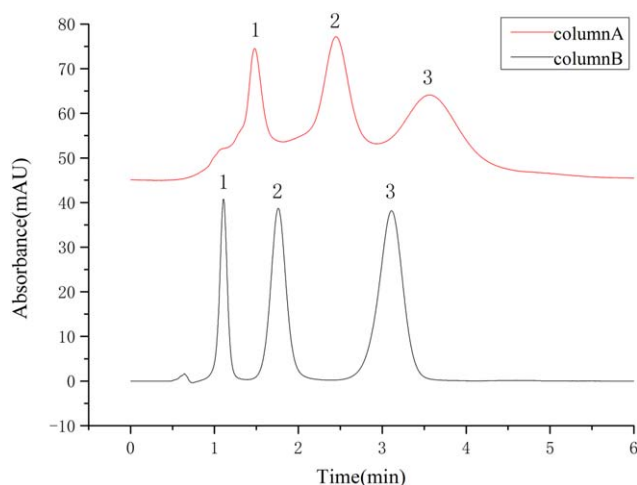


Figure 8. Separation of three alkaline compounds on column A and column B in HPLC; separation conditions: ACN/water (65/35, v/v) at a flow rate of 1 mL/min; detection wavelength, 254 nm; the analytes were (1) *p*-nitroaniline, (2) 1-naphthylamine, and (3) diphenylamine. [Color figure can be viewed in the online issue, which is available at wileyonlinelibrary.com.]

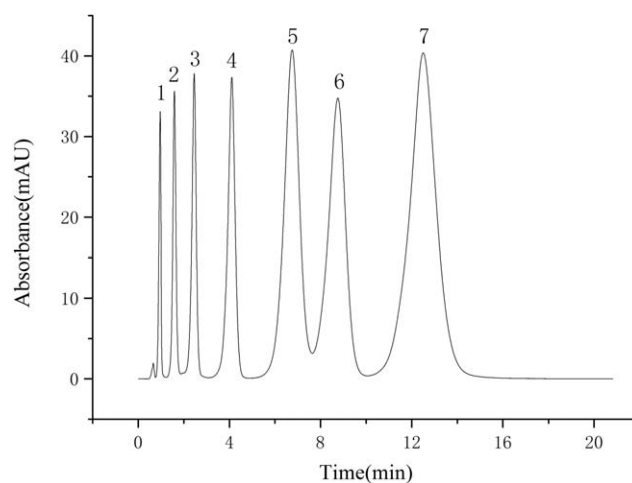


Figure 9. Separation of seven compounds on column B in HPLC; separation conditions: ACN/water (50/50, v/v) at a flow rate of 1 mL/min; detection wavelength, 254 nm; the analytes were (1) *o*-nitrobenzoic acid, (2) *p*-nitroaniline, (3) benzene, (4) chlorobenzene, (5) diphenylamine, (6) *p*-aminodiphenylimide, and (7) acenaphthylene.

(RSDs) of the retention times using benzene, diphenyl, and phenanthrene as test compounds. The RSD of the retention time column-to-column and run-to-run was less than 2.31% ($n = 5$) and 1.63% ($n = 5$), respectively. These results suggested that the method had a good reproducibility, and the monolith was stable.

CONCLUSIONS

In this study, a nanodiamond-based composite monolithic column was prepared by redox initiation and characterized for separation of small molecules in RP-HPLC mode. The addition of functionalized nanodiamond improved the separation performance, resolution, and column efficiency of the resulting monolithic column in the separation of aromatic compounds. The mixture of acidic, alkaline, and neutral compounds could be separated at the same time. Moreover, the present composite monolith exhibited a uniform skeleton microstructure, thermostability, low pressure, and good mechanical stability and permeability. The results suggested that the proposed nanodiamond-based composite monolith could be used as a promising, simple stationary phase to separate small molecules in HPLC.

ACKNOWLEDGMENTS

This work was supported by the National Natural Science Foundation of China (No. 21175031, 21575033), the Natural Science Foundation of Hebei Province (No. B2013201082), and the Natural Science Foundation of Hebei University (No. 2014-05).

REFERENCES

1. Aris, A.; Shojaei, A.; Bagheri, R. *Ind. Eng. Chem. Res.* **2015**, *54*, 8954.
2. Krueger, A. *J. Mater. Chem.* **2008**, *18*, 1485.
3. Bitounis, D.; Ali-Boucetta, H.; Hong, B. H.; Min, D.-H.; Kostarelos, K. *Adv. Mater.* **2013**, *25*, 2258.
4. Lacerda, L.; Bianco, A.; Prato, M.; Kostarelos, K. *Adv. Drug Delivery Rev.* **2006**, *58*, 1460.
5. Li, Y.; Zhu, Z.; Yu, J.; Ding, B. *ACS Appl. Mater. Interfaces* **2015**, *7*, 13538.
6. Badziag, P.; Verwoerd, W. S.; Ellis, W. P.; Greiner, N. R. *Nature* **1990**, *343*, 244.
7. Mochalin, V. N.; Gogotsi, Y. *Diamond Relat. Mater.* **2015**, *58*, 161.
8. Krueger, A.; Lang, D. *Adv. Funct. Mater.* **2012**, *22*, 890.
9. Pastrana-Martínez, L. M.; Morales-Torres, S.; Carabineiro, S. A. C.; Buijnsters, J. G.; Faria, J. L.; Figueiredo, J. L.; Silva, A. M. T. *ChemPlusChem* **2013**, *78*, 801.
10. Zhang, J.; Su, D. S.; Blume, R.; Schllögl, R.; Wang, R.; Yang, X.; Gajović, A. *Angew. Chem. Int. Ed.* **2010**, *49*, 8640.
11. Maze, J. R.; Stanwix, P. L.; Hodges, J. S.; Hong, S.; Taylor, J. M.; Cappellaro, P.; Jiang, L.; Dutt, M. V. G.; Togan, E.; Zibrov, A. S.; Yacoby, A.; Walsworth, R. L.; Lukin, M. D. *Nature* **2008**, *455*, 644.
12. Zhang, Q.; Mochalin, V. N.; Neizel, I.; Knoke, I. Y.; Han, J.; Klug, C. A.; Zhou, J. G.; Lelkes, P. I.; Gogotsi, Y. *Biomaterials* **2011**, *32*, 87.
13. Baklavaridis, A.; Zuburtikudis, I.; Panayiotou, C. *Polym. Eng. Sci.* **2015**, *55*, 1856.
14. Wu, R.; Hu, L.; Wang, F.; Ye, M.; Zou, H. *J. Chromatogr. A* **2008**, *1184*, 369.
15. Hilder, E. F.; Svec, F.; Fréchet, J. M. J. *J. Chromatogr. A* **2004**, *1044*, 3.
16. Bristow, P. A.; Knox, J. H. *Chromatographia* **1977**, *10*, 279.
17. Nikam, P. S.; Shirsat, L. N.; Hasan, M. *J. Chem. Eng. Data* **1998**, *43*, 732.
18. Ping, G.; Zhang, L.; Zhang, L.; Zhang, W.; Schmitt-Kopplin, P.; Kettrup, A.; Zhang, Y. *J. Chromatogr. A* **2004**, *1035*, 265.
19. Martín, R.; Álvaro, M.; Herance, J. R.; García, H. *ACS Nano* **2010**, *4*, 65.
20. Martín, R.; Heydorn, P. C.; Alvaro, M.; García, H. *Chem. Mater.* **2009**, *21*, 4505.
21. Ueki, Y.; Umemura, T.; Iwashita, Y.; Odake, T.; Haraguchi, H.; Tsunoda, K. *J. Chromatogr. A* **2006**, *1106*, 106.
22. Shu, S.; Kobayashi, H.; Okubo, M.; Sabarudin, A.; Butsugan, M.; Umemura, T. *J. Chromatogr. A* **2012**, *1242*, 59.
23. Bai, X.; Liu, H.; Wei, D.; Yang, G. *Talanta* **2014**, *119*, 479.
24. Hao, M.; Zhong, J.; Li, R.; Li, H.; Bai, L.; Yang, G. *Anal. Methods* **2014**, *6*, 2655.

SGML and CITI Use Only
DO NOT PRINT

